

# Three-Dimensional Nonlinear Lattices: From Oblique Vortices and Octupoles to Discrete Diamonds and Vortex Cubes

R. Carretero-González<sup>1</sup>, P.G. Kevrekidis<sup>2</sup>, B.A. Malomed<sup>3</sup> and D.J. Frantzeskakis<sup>4</sup>

<sup>1</sup> *Nonlinear Dynamical Systems Group, Department of Mathematics & Statistics, San Diego State University, San Diego CA, 92182-7720*

<sup>2</sup> *Department of Mathematics and Statistics, University of Massachusetts, Amherst MA 01003-4515, USA*

<sup>3</sup> *Department of Interdisciplinary Studies, Faculty of Engineering, Tel Aviv University, Tel Aviv 69978, Israel*

<sup>4</sup> *Department of Physics, University of Athens, Panepistimiopolis, Zografos, Athens 15784, Greece*

We construct a variety of novel localized states with distinct topological structures in the 3D discrete nonlinear Schrödinger equation. The states can be created in Bose-Einstein condensates trapped in strong optical lattices, and crystals built of microresonators. These new structures, most of which have no counterparts in lower dimensions, range from purely real patterns of dipole, quadrupole and octupole types to vortex solutions, such as “diagonal” and “oblique” vortices, with axes oriented along the respective directions  $(1, 1, 1)$  and  $(1, 1, 0)$ . Vortex “cubes” (stacks of two quasi-planar vortices with like or opposite polarities) and “diamonds” (discrete skyrmions formed by two vortices with orthogonal axes) are constructed too. We identify stability regions of these 3D solutions and compare them with their 2D counterparts, if any. An explanation for the stability/instability of most solutions is proposed. The evolution of unstable states is studied as well.

*Introduction.* In the past two decades an explosion of activity has been observed in the study of intrinsic localized modes (ILMs, *alias* discrete solitons) in nonlinear dynamical lattices, especially due to the ability of such modes to act as energy “hot spots” [1]. The relevance of ILMs has been demonstrated in problems ranging from arrays of nonlinear-optical waveguides [2] and photonic crystals [3], to Bose-Einstein condensates (BECs) trapped in optical lattices (OLs) [4] and Josephson-junction ladders [5].

A universal model, which may arise as an envelope approximation from most of the complex nonlinear equations on the lattice and also as direct physical model for the BECs [4] and optical waveguiding arrays [6, 7], is the discrete nonlinear Schrödinger (DNLS) equation [8]. On top of its significance to applications, the DNLS equation itself is a fundamentally interesting dynamical model. In the 3D case, its direct physical realization is provided, as mentioned above, by BECs trapped in strong OLs [4]. Waveguide arrays, however, cannot be described by a 3D discrete model, since the evolution variable in the optical media is a spatial coordinate, while the temporal variable, which effectively plays the role of an additional quasi-spatial one, cannot be discrete. Nevertheless, another physical realization of the 3D DNLS equation may be provided by a crystal built of microresonators [9].

The study of the 3D continuum NLS equation, including a 3D [10] or quasi-2D [11] OL, and of the DNLS model proper [12], has started recently, becoming increasingly accessible to numerical computations. As a result, the first coherent structures, such as discrete vortices of the topological charge (vorticity)  $S = 1, 2$  and  $3$ , were identified and their stability was investigated. The aim of the present work is to study a large variety of novel localized 3D structures in the DNLS equation, many of which turn out to be stable. In particular, we construct states which include, first, dipoles with the axis oriented along a lattice bond, or along a planar diagonal, or along a 3D diago-

nal (we call them, respectively, “straight”, “oblique”, and “diagonal” dipoles). Next, we construct quadrupole and octupole states, that, similarly to the dipoles, are real solutions. More sophisticated structures are also presented, namely “vortex cubes” (concatenations of two straight vortices with the same or opposite charges centered on parallel planes), oblique and diagonal vortices, and “vortex diamonds”, formed by a crossed pair of vortices with orthogonal axes. Apart from the straight and oblique dipoles and quadrupoles, these ILMs have no counterparts in 2D lattices.

To present the results, we first introduce the model, and then report systematic numerical results for the shape and stability of the new localized states. This is followed by conclusions, which include an explanation for the stability and instability of the majority of patterns found in this work.

*The Model.* We consider the DNLS equation on the cubic lattice with a coupling constant  $C$  [12],

$$i\dot{\phi}_{l,m,n} + C\Delta\phi_{l,m,n} + |\phi_{l,m,n}|^2\phi_{l,m,n} = 0, \quad (1)$$

with  $\dot{\phi} = d\phi/dt$ , and the discrete Laplacian is  $\Delta\phi_{l,m,n} \equiv \phi_{l+1,m,n} + \phi_{l,m+1,n} + \phi_{l,m,n+1} + \phi_{l-1,m,n} + \phi_{l,m-1,n} + \phi_{l,m,n-1} - 6\phi_{l,m,n}$ . Solutions are looked for as  $\phi_{l,m,n} = u_{l,m,n} \exp(i\Lambda t)$  with a frequency  $-\Lambda$  (or the chemical potential in the context of BEC), where the stationary functions  $u_{l,m,n}$  obey the equation

$$\Lambda u_{l,m,n} = C\Delta u_{l,m,n} + |u_{l,m,n}|^2 u_{l,m,n}. \quad (2)$$

Profiles used as an initial guess for the fixed-point iteration converging to solutions displayed below, were based on the form of the respective solutions (for the same  $\Lambda$ ) in the anti-continuum (AC) limit,  $C = 0$ . Once solutions to Eq. (2) have been obtained, the linear-stability analysis is performed for a perturbed solution [12],  $\phi_{l,m,n} = [u_{l,m,n} + \epsilon (a_{l,m,n} e^{\lambda t} + b_{l,m,n} e^{\lambda^* t})] e^{i\Lambda t}$ , where  $\epsilon$  is an infinitesimal amplitude of the perturbation, and  $\lambda$  is its

eigenvalue. The Hamiltonian nature of the system dictates that if  $\lambda$  is an eigenvalue, then so are  $-\lambda$ ,  $\lambda^*$  and  $-\lambda^*$  (in the stable case,  $\lambda$  is imaginary, hence this symmetry yields only two different eigenvalues,  $\lambda$  and  $-\lambda$ ). The stationary solution is unstable if at least one pair of the eigenvalues features nonvanishing real parts.

*Results.* We start by constructing purely real solutions of the dipole type (in lower-dimensional models, solitons of this type were considered in Refs. [13, 14]). Figure 1 displays generic examples of “tight” dipoles with adjacent excited sites (i.e., the separation between them is  $d = 1$ , in the corresponding units) and three possible orientations relative to the lattice: *straight* (along a lattice’s bond), (a), *oblique* (along a planar diagonal), (b), and *diagonal* (along a 3D diagonal), (c). In this figure and below, unless stated otherwise, we show a typical case admitting stable solutions, with  $C = 0.1$  and  $\Lambda = 2$ . The borders of the stability windows,  $0 \leq C \leq C_{\text{dip}}^{(3D,d)}$ , for the three types (straight, oblique and diagonal) of the dipoles are given by  $C_{\text{dip-str}}^{(3D,1)} = 0.23013 \pm \delta C$ ,  $C_{\text{dip-obl}}^{(3D,1)} = 0.53666 \pm \delta C$ , and  $C_{\text{dip-dia}}^{(3D,1)} = 0.73084 \pm \delta C$ , where the error margin is  $\delta C = 0.00001$  for all the results presented in this work (unless indicated otherwise). We observe that the diagonal dipole in Fig. 1(c) remains stable in a larger interval than its oblique counterparts in Fig. 1(b) that, in turn, is more stable than the diagonal one in Fig. 1(c). It is also possible to construct dipole solutions corresponding to  $d = 2$ , with excited sites separated by a single nearly empty site. Such dipole solutions (not depicted here) have larger stability windows than their “tight” ( $d = 1$ ) counterparts:  $C_{\text{dip-str}}^{(3D,2)} = 0.66722$ ,  $C_{\text{dip-obl}}^{(3D,2)} = 1.08024$ , and  $C_{\text{dip-dia}}^{(3D,2)} = 1.31356$ . As seen in Fig. 1(h),  $C_{\text{dip}}^{(3D,d)}$  further increases with the separation distance  $d$ , approaching the stability threshold of the fundamental (single-site-based) discrete soliton,  $C_{\text{dip}}^{(3D,\infty)} \equiv C_{\text{fund}}^{(3D)} = 2.009 \pm 0.001$  [12], see the horizontal dashed line in the figure. It can also be found that the same relations,  $0 < C_{\text{dip-str}}^{(3D,d)} < C_{\text{dip-obl}}^{(3D,d)} < C_{\text{dip-dia}}^{(3D,d)}$ , as found for  $d = 1$ , are valid for all  $d$ , see Fig. 1(h). Another relevant comparison is with dipoles in the 2D DNLS model, which were studied in Ref. [15]. The comparison shows that the dipole soliton of the oblique and straight types, which have their counterparts in the 2D case, are less stable, although not drastically, than those counterparts:  $C_{\text{dip-str}}^{(3D,1)} = 0.23013 < C_{\text{dip-str}}^{(2D,1)} = 0.245 \pm 0.005$  for  $\Lambda = 2$ . The weaker stability of the 3D structures is explained by the analogy with the multidimensional continuum NLS equation, where all the solitons are destabilized by collapse, which is, respectively, *weak* and *strong* in the 2D and 3D cases [16].

Quadrupole and octupole solitons are also shown in Fig. 1. The quadrupole is based on four contiguous sites (so that we prescribe  $d = 1$  to this structure too) which form a square in the plane, Fig. 1(d). It was found to be stable for  $C < C_{\text{quad}}^{(3D,1)} = 0.13836$ , while its 2D analog

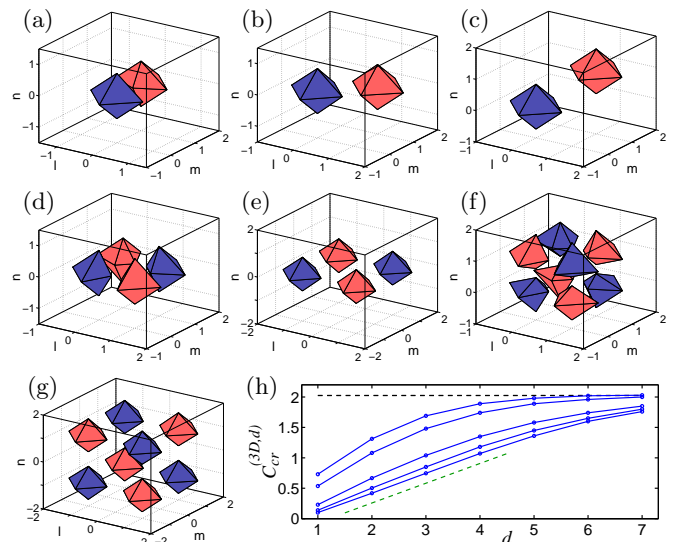


FIG. 1: (Color online) Stable multipoles. The top row depicts stable “tight” dipoles (with  $d = 1$ ): (a) straight, (b) oblique, and (c) diagonal ones. (d) and (e): Quadrupoles in the  $n = 0$  plane, with the internal separation  $d = 1$  and  $d = 2$ , respectively. (f) and (g): Octupoles with  $d = 1$  and  $d = 2$ . Panel (h) displays the stability threshold  $C_{\text{cr}}^{(3D,d)}$  as a function of the internal distance  $d$  for (from top to bottom) diagonal, oblique, and straight dipoles, octupoles and quadrupoles. The horizontal dashed line corresponds to the stability threshold for the fundamental discrete soliton,  $C_{\text{fund}}^{(3D)} \approx 2$ . Note that, for the quadrupole (the bottom graph),  $C_{\text{quad}}^{(3D,d)}$  behaves linearly for small  $d$  (see the dashed line with slope 0.325 for guidance). In panels (a)-(g), level contour corresponding to  $\text{Re}(u_{l,m,n}) = \pm 0.5$  are shown in blue and red (dark gray and gray, in the black-and-white version), respectively. All these states are *stable* (for the case shown, with  $\Lambda = 2$  and  $C = 0.1$ ).

has  $C_{\text{quad}}^{(2D,1)} = 0.1485 \pm 0.0005$  [17]. In this case, as well as it was with the dipoles, the 2D configurations tend to be slightly more stable than their 3D siblings. The octupole is shown in panel 1(f); it is based on a set of eight continuous sites (therefore it is also assigned  $d = 1$ ) forming a cubic cell in the 3D lattice. It is stable in the interval  $C < C_{\text{oct}}^{(3D,1)} = 0.10030$ , which is smaller than the above ones for the quadrupoles and dipoles. Similar to the dipoles, multipoles can also “swell” by inserting unpopulated sites between the excited ones. The resulting stability intervals for  $d = 2$  are larger than their  $d = 1$  counterparts:  $C_{\text{quad}}^{(3D,2)} = 0.503232$  and  $C_{\text{oct}}^{(3D,2)} = 0.418411$ , see Figs. 1(e) and (g), respectively. It is relevant to mention that all the newly found structures have their stability limits lower than those for the fundamental (single-site-based) discrete soliton,  $C_{\text{fund}}^{(3D)} = 2.009 \pm 0.001$  [12], see Fig. 1(h).

Stable dipoles have one pair of imaginary eigenvalues in their perturbation-mode spectrum, that, with the increase of  $C$ , collides with the continuous spectrum, which leads to the destabilization. On the other hand, stable quadrupoles have three such pairs (two of them form a

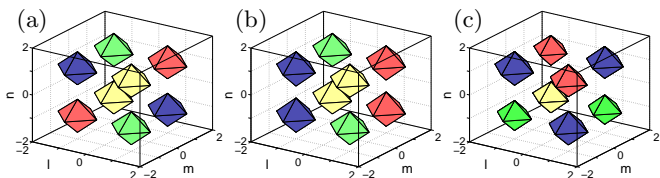


FIG. 2: (Color online) Vortex cubes for  $\Lambda = 2$  and  $C = 0.1$ . Panel (a) shows a *stable* vortex cube, built of two quasi-planar vortices, set in the planes  $n = \pm 1$ , with equal vorticities,  $S_1 = S_2 = 1$ , and a phase shift of  $\pi$ . Panel (b) shows an unstable cube formed by vortices with opposite charges,  $S_1 = -S_2$  and panel (c) shows a snapshot (at  $t = 200$ ) of its evolution, clearly demonstrating that the phase coherence between sites forming the pattern is lost. The real level contours are as in Fig. 1, and the imaginary ones,  $\text{Im}(u_{l,m,n}) = \pm 0.5$ , are shown by green and yellow (light and very light gray, in the black-and-white version) hues, respectively.

doublet for small  $C$ ), and the octupoles have seven (six of which form two triplets for small  $C$ ). More generally, the number of potentially unstable eigenvalue pairs is  $N - 1$ , where  $N$  is the number of sites on which the structure is based [18].

The next novel type of a 3D discrete soliton, with no lower-dimensional counterpart, is a “vortex cube”, which is built as a stack of two quasi-planar vortices with equal topological charges  $S_1 = S_2 = 1$  and a phase shift  $\Delta\phi = \pi$ , separated by an empty layer, so that it has  $d = 2$ . Figure 2(a) shows real and imaginary parts of the vortex-cube lattice field. Such a state is stable for  $0 \leq C \leq C_{\text{cub},\pi}^{(3\text{D},2)} = 0.56324$ . On the contrary to this, a vortex cube built as a stack of two in-phase vortices, with  $\Delta\phi = 0$ , is *always unstable*, through three real eigenvalue pairs. Further, Fig. 2(b) shows a similar stack, but composed of two vortices with opposite charges,  $S_1 = -S_2 = 1$ . This configuration is *always unstable* as well, due to a real eigenvalue pair. In this case, the instability manifests itself as a symmetry breaking between the two planes and, hence, the phase coherence of the entire pattern is eventually lost, see Fig. 2(c).

Another 3D object, with no lower-dimensional analog either, is a vortex with the axis directed along the diagonal of the cubic lattice, i.e., the vector  $(1, 1, 1)$ . Figure 3(a) shows such a “diagonal vortex” constructed by a continuation procedure starting, in the AC limit, with the following distribution of local phases:  $\phi_{l,m,n} = 2\pi S k / 6$  ( $k = 0, 1, 2, \dots, 5$ ), for the sites that lie in a plane orthogonal to the axial (diagonal) direction:  $(1, -1, 0)$ ,  $(0, -1, 1)$ ,  $(-1, 0, 1)$ ,  $(-1, 1, 0)$ ,  $(0, 1, -1)$ ,  $(1, 0, -1)$ . Obviously, this phase pattern bears the vorticity  $S$  ( $S = 1$  in Fig. 3). However, the diagonal vortex turns out to be *always unstable*, due to three real eigenvalue pairs, and it eventually settles to a single-site-based soliton.

One more species of discrete vortices that may exist solely in the 3D lattice is an “oblique” one, shown in Figs. 3(b)-(c), with the axis’ directed along  $(1, 1, 0)$ . In the AC limit, the solution is carried by the array of sites  $(1, -1, 0)$ ,  $(1, -1, 1)$ ,  $(0, 0, 1)$ ,  $(-1, 1, 1)$ ,  $(-1, 1, 0)$ ,

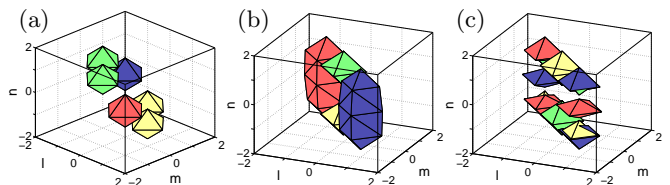


FIG. 3: (Color online) Diagonal and oblique vortices. Panel (a) shows an unstable “diagonal” vortex, with the axis along the direction  $(1, 1, 1)$ , for  $\Lambda = 2$  and  $C = 0.1$ . Panel (b) shows an unstable oblique vortex with the axis oriented along the direction  $(1, 1, 0)$ , and panel (c) shows a *stable* oblique vortex of a modified form (see text) for  $\Lambda = 2$  and  $C = 0.01$ .

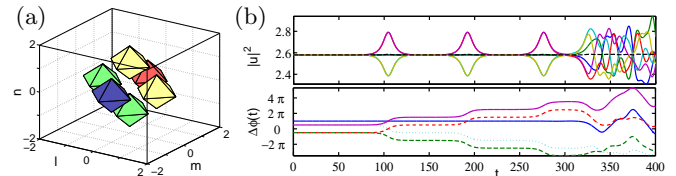


FIG. 4: (Color online) The vortex diamond (discrete skyrmion) for  $\Lambda = 2$  and  $C = 0.1$ . Panel (a) displays an unstable “diamond”, and panel (b) depicts its evolution, in terms of the field’s magnitude (top) and phase (bottom) at the main six lattice sites. Initially ( $t < 300$ ), pairs of sites (opposite vertices of the diamond) cyclically change the phase, and subsequently ( $t > 350$ ) the phase coherence is lost and the field magnitude oscillates erratically about its initial level.

$(-1, 1, -1)$ ,  $(0, 0, -1)$ , and  $(1, -1, -1)$ , with the phases at them  $S \cdot (0, \alpha, \pi/2, \alpha + \pi/2, \pi, \alpha + \pi, 3\pi/2, \alpha + 3\pi/2)$ , where  $\alpha \equiv \tan^{-1}(1/\sqrt{2})$ . Figure 3(b) depicts such an oblique vortex, which, in this form, is found to be *always unstable*, similar to the diagonal vortex. Nonetheless, the oblique vortex can be stabilized in a modified form, by introducing a sign shift at the intermediate edge sites [i.e.,  $(0, 0, 1)$ ,  $(-1, 1, 0)$ ,  $(0, 0, -1)$  and  $(1, -1, 0)$ ], see Fig. 3(c). This sign change avoids contiguous sites with the same phase and does not alter the vortex’ topological charge, which remains 1. The modified oblique vortex is stable in a small interval,  $C < C_{\text{vor-obl}}^{(3\text{D})} = 0.0104$ .

Finally, motivated by the concept of skyrmions [19], which are distinguished by two topological charges associated with closed contours in two perpendicular planes, we have constructed one more type of vortex structures in the 3D lattice, viz., a “diamond” shown in Fig. 4(a). It is built as a vortex cross, i.e., a nonlinear superposition of two straight site-centered  $S = 1$  vortices, with their axes directed along two orthogonal directions. The stability analysis shows that, although the diamond has three imaginary (stable) eigenvalue pairs, it is *always unstable* due to a real eigenvalue pair. In direct simulations, its instability manifests itself in a rather intriguing manner, see Fig. 4(b). At  $t \approx 100$ , two pairs of opposite vertices of the diamond change phases (one by  $+\pi/2$  and the other by  $-\pi/2$ ) and suffer a momentary magnitude change. After this, the diamond remains stable until  $t \approx 200$ , when the same pairs of sites suffer an-

other phase shift (in the same direction). This process repeats itself almost periodically until (at  $t \approx 340$ ) the diamond, after 4 shifts, returns back to its original phase distribution. Subsequently, the phase shifts accelerate and phase coherence is finally lost. Simultaneously, amplitude variations of  $\pm 10\%$  get accumulated, see the top panel of Fig. 4(b). Eventually, the solution degenerates into a plain single-site-based soliton.

*Conclusions and discussion.* We have introduced several novel species of topologically structured discrete solitons in 3D dynamical lattices, using the paradigm of the discrete nonlinear Schrödinger equation. The solutions have been constructed starting from properly chosen anti-continuum approximations, and their linear stability was studied through the computation of the relevant eigenvalues. Previously, only the fundamental single-site-based solitons and straight vortices, with the axis directed along a lattice bond, were known. We have found three species of dipoles, which differ by the orientation relative to the lattice, quadrupoles and octupoles, vortex cubes (stacked dual-vortex patterns), diagonal and oblique vortices, and “diamonds” (vortex crosses or discrete skyrmions). Except for the straight and oblique dipoles and quadrupoles, the patterns obtained are endemic to the 3D lattice setting, having no counterparts in lower dimensions.

Apart from the diagonal vortices and “diamonds”, all the patterns constructed above have stability regions below a critical value of the coupling parameter. It is pos-

sible to explain the stability/instability of all the structures that may be realized as bound states of two simpler objects, viz., dipoles, quadrupoles (bound states of two dipoles with opposite orientations), octupoles (bound states of two quadrupoles), and vortex cubes. Indeed, a known general principle is that a bound state pinned by the lattice may be stable only if the coupled objects *repel* each other [15, 20] (i.e., have a phase difference of  $\pi$  between their building blocks). This explains the existence of stability regions for multipoles of all types. Similarly, considering the interaction between constituent quasi-planar vortices, one may understand the stability and instability of vortex cubes of the types shown in Figs. 2(a) and 2(b), respectively. Following this principle, it is also possible to predict the stability of more exotic 3D patterns such as bound states of two oblique or diagonal dipoles, or octupoles constructed of two such states. In those cases when the 3D structures have 2D counterparts, viz., straight and oblique dipoles and quadrupoles, their stability regions are narrower than in the 2D case, which is explained by a stronger trend to collapse in three dimensions.

Future challenges involve semi-analytical investigation of such solutions via Lyapunov-Schmidt theory, and identification of their stability by means of methods similar to those developed for the 1D and 2D cases [18]. On the experimental side, it may be interesting to create such structures in BEC loaded into a strong optical lattice.

- 
- [1] S. Aubry, *Physica* **103D**, 201 (1997); S. Flach and C.R. Willis, *Phys. Rep.* **295**, 181 (1998); D.N. Christodoulides F. Lederer, and Y. Silberberg, *Nature* **424**, 817 (2003); D.K. Campbell, S. Flach, and Y.S. Kivshar, *Phys. Today*, January (2004), p. 43.
  - [2] see e.g., A.A. Sukhorukov, Y.S. Kivshar, H.S. Eisenberg, and Y. Silberberg, *IEEE J. Quant. Elect.* **39**, 31 (2003); U. Peschel *et al.*, *J. Opt. Soc. Am. B* **19**, 2637 (2002).
  - [3] S. F. Mingaleev and Y.S. Kivshar, *Phys. Rev. Lett.* **86**, 5474 (2001).
  - [4] A. Trombettoni and A. Smerzi, *Phys. Rev. Lett.* **86**, 2353 (2001); F.Kh. Abdullaev *et al.*, *Phys. Rev.* **A64**, 043606 (2001); F.S. Cataliotti *et al.*, *Science* **293**, 843 (2001); A. Smerzi *et al.*, *Phys. Rev. Lett.* **89**, 170402 (2002); G.L. Alfimov, P.G. Kevrekidis, V.V. Konotop, and M. Salerno, *Phys. Rev. E* **66**, 046608 (2002); R. Carretero-González and K. Promislow, *Phys. Rev. A* **66** 033610 (2002).
  - [5] P. Binder *et al.*, *Phys. Rev. Lett.* **84**, 745 (2000); E. Trías *et al.*, *Phys. Rev. Lett.* **84**, 741 (2000).
  - [6] D.N. Christodoulides and R.I. Joseph, *Opt. Lett.* **13**, 794 (1988); A. Aceves *et al.*, *Opt. Lett.* **19**, 1186 (1994).
  - [7] H.S. Eisenberg *et al.*, *J. Opt. Soc. Am. B* **19**, 2938 (2002); J. Meier *et al.*, *Phys. Rev. Lett.* **91**, 143907 (2003).
  - [8] P.G. Kevrekidis, K.Ø. Rasmussen and A.R. Bishop, *Int. J. Mod. Phys. B* **15**, 2833 (2001).
  - [9] J.E. Heebner and R.W. Boyd, *J. Mod. Opt.* **49**, 2629 (2002); P. Chak *et al.*, *Opt. Lett.* **28**, 1966 (2003).
  - [10] B.B. Baizakov, V.V. Konotop, and M. Salerno, *J. Phys. B* **35**, 5105 (2002); B.B. Baizakov, B.A. Malomed, and M. Salerno, *Europhys. Lett.* **63**, 642 (2003).
  - [11] B.B. Baizakov, B.A. Malomed, and M. Salerno, *Phys. Rev. A* **70**, 053613 (2004).
  - [12] P.G. Kevrekidis, B. Malomed, D.J. Frantzeskakis and R. Carretero-González, *Phys. Rev. Lett.* **93**, 080403 (2004).
  - [13] P.G. Kevrekidis, B.A. Malomed, A.R. Bishop, and D.J. Frantzeskakis, *Phys. Rev. E* **65**, 016605 (2002).
  - [14] J. Yang *et al.*, *Opt. Lett.* **29**, 1662 (2004).
  - [15] P.G. Kevrekidis, B.A. Malomed, and A.R. Bishop, *J. Phys. A* **34**, 9615 (2001).
  - [16] C. Sulem and P.L. Sulem, *The Nonlinear Schrödinger Equation*, Springer-Verlag (New York, 1999).
  - [17] P.G. Kevrekidis, B.A. Malomed, Z. Chen, and D.J. Frantzeskakis, *Phys. Rev. E* **70**, 056612 (2004).
  - [18] D.E. Pelinovsky, P.G. Kevrekidis, and D.J. Frantzeskakis *nlin.PS/0411016* and *nlin.PS/0410005*.
  - [19] T.H.R. Skyrme, *Proc. Roy. Soc. London A* **260**, 127 (1961).
  - [20] T. Kapitula, P.G. Kevrekidis, and B.A. Malomed, *Phys. Rev. E* **63**, 036604 (2001).